Romanian Reports in Physics, Vol. 67, No. 2, P. 508–522, 2015

THE INFLUENCE OF GAMMA RAYS AND PROTONS AFFECTED OPTICAL MEDIA ON A REAL GAUSSIAN LASER BEAM PARAMETERS

M. R. IOAN[1], I. GRUIA[2*], G. V. IOAN[1], L. RUSEN[3], C. D. NEGUT[1], P. IOAN[1]

[1]"Horia Hulubei" National Institute of Physics and Nuclear Engineering - IFIN HH, 30 Reactorului Str., 077125 Măgurele, Bucharest, Romania
[2]University of Bucharest, Faculty of Physics, 405 Atomiştilor Str., 077125 Măgurele - Bucharest, Romania; *Corresponding author: gruia_ion@yahoo.com
[3]ISOTEST Laboratory, National Institute for Lasers, Plasma and Radiation Physics, 409 Atomiştilor Str., 077125 Măgurele, Bucharest, Romania

Received April 21, 2014

Abstract. In this paper it was applied an indirect diagnostic technique for studying optical samples, using a Gaussian laser beam as a testing instrument. We had in mind to study the influence of the changes, due to ionizing radiation, on the energetic and propagation parameters for both the artificial laser beam and the real emergent one. To be more specific, we investigated, as a side by side view, the changes due to the absorption centers or to other damages produced by ionizing radiation on two types of borate glass, by studying the modifications produced to the test beam. In principal, beside the change of the transmission proprieties, we can expect to changes in the energetic and spatial profile of the test beam. Gamma irradiation was performed in air using a gamma chamber equipped with a ^{60}Co source. Irradiation temperature was up to 34^{0}C. Measured absorbed dose was 24.4kGy which was accumulated at a constant dose rate of 6.2kGy/h. For dose measurement, an ECB dosimeter system with an average measurement uncertainty of 2.5% was used. 12MeV protons irradiation was performed in air using a beam with a flow current of about 5nA using a TANDEM linear type accelerator. Irradiation temperature was up to 40^{0}C. Estimated absorbed dose, by calculations, was of about 36kGy. The changes of the energetic and propagation parameters were highlighted using a continuous beam He-Ne laser, having a 633nm wavelength. The characterization of the beam, before and after passing the blank sample and then the irradiated ones, was done in conformity with the International Standards ISO 11554 and ISO 11146. The main purpose of this energetic and spatial characterization of the laser beam was to see if there are or not changes in the internal structure of the irradiated glass samples, changes that can directly affect these parameters. There were highlighted modifications of these two main parameters, in the frame of the measuring uncertainties, using an experimental setup containing the following USA made components: a type 05 - LHP - 991 He-Ne laser - CVI Melles Griot, a PowerMax - USB PM30 UV–VIS power-meter and a GRAS20 beam analyser with the BeamGage dedicated software from Ophir Optronics.

Key words: ISO-Standard, He-Ne laser, optical glass, gamma rays, protons, asymmetry, astigmatism.

1. INTRODUCTION

Optical components based on transparent optical glass (optical windows, lenses, protective covers) similar to those used in some optical systems related to nuclear technologies are optical affected by the exposure to ionizing radiations. The interaction of ionizing radiation with the glass structure can produce effects as are the excitation, ionization and displacement of constituent atoms, and sometimes the production of free radicals. Endowed with electric charge, protons have a small possibility of penetrating into the nucleus and interact with it. During the interaction, the protons do not present a major scattering effect. Being heavier comparing to electrons makes a small number of scattering acts to be produced when interacting with atomic nuclei. Atomic electrons have no influence on the scattering of the particles from the incident beam, but receive only a fraction of the protons energy. In general, protons passing through the substance is characterized both by energy loss per unit and total physical process until their stop [1, 2] – Tabel 1 (col. 3, 4). Monte Carlo simulation using SRIM program [3] provides us a graphic picture of the interaction. It was noted that for over 12MeV energy protons, the projected range for our two types of samples is less than 1 mm (Table 1 – col. 3). At the same time, it is also revealed their way of releasing energy during their trajectory, in terms of speed. The attenuation effect is more prominent towards the end of the trajectory, when protons have a very low speed. The total attenuation study in these samples shows that the effect of optical degradation on a multi-component optical system is present only in the first component of the optical chain. So, when charged particles (*i.e*. protons) are involved, optical protection may be achieved by placing in front of the first component of a 2 mm optical glass cover.

Unlike the interaction effect of protons on optical multi-component systems, for gamma radiation there are three important effects that are taken into account: photoelectric effect, Compton effects and the electron-positron pairs creation effect [4, 5, 6]. For the average energy of 1.25MeV of ^{60}Co, the predominant effect is the Compton one. The absorption mechanism of gamma radiation is totally different from the one of the particles (*i.e*. protons), because photons have no electric charge (no electrostatic interactions), and no rest mass. For this reason, gamma radiation is not slowed down by substance, but only absorbed or scattered. In these interaction processes, photons give some of their energy, but are also strongly scattered and backscatter. Some of the photons are absorbed in the substance, but the rest can be found at the end of their interaction, so, the ones passed thru will affect the other components of optical chain, but increasingly less. For gamma radiation, it can be also used a cover glass optical protection, but having a substantial thickness. This thickness will have an additional influence on the laser beam energy and propagation parameters. In this case, corrective measures are required to be applied for the laser parameters. A characteristic of gamma radiation interacting with matter is the half thickness (cm):

$$d_{0.5} = \frac{0.693}{a \times \rho}, \tag{1}$$

where $a = \frac{\mu}{\rho}$ – overall mass attenuation/absorption coefficient [g/cm^2]; ρ – material density [g/cm^3].

Results based on equation (1) are shown in Table 1 (col.2).

Table 1

The dose rate halving thickness, the distance and the proton beam energy loss

Glass type	1.25MeV Gamma radiation – ^{60}Co	12MeV protons	
	The halving thickness of the half (cm)	Projected range (mm)	The energy lost during the trajectory (MeV)
BK-7	4.89	0.812	7.81
TEMPAX	5.49	0.935	6.77

During the attenuation process, absorbed dose flow (attenuated) gradually decreases and no matter how thick the attenuator will be, it will not be able to achieve total beam attenuation. Photon interaction occurs according to the following exponential law (2):

$$D = D_0 \times \mathrm{e}^{-a \times \rho \times d_{0.5}}. \tag{2}$$

Total mass attenuation and absorption coefficient in tested glass (1.25MeV mean energy gamma) was obtained by the simulation program XCOM [7]. Using equation (2), the dependence of attenuation and absorbed dose rate as a function of the sample thickness was revealed graphically (Fig.1). Figure 1 shows the variation of absorbed dose rate and attenuation for a number of 7 glass thicknesses (BK-7 glass (10mm) and Tempax (2 mm)). In both types of samples, the relative variation of the absorption is between (30÷33)% and the one of the attenuation is between (53÷57)%.

We can observe a small difference between the samples, of about 3% for absorption and 4% for attenuation. We can also notice, that for each sample tested, there is a notable difference between the relative variation of the absorption and attenuation (23÷24)%. In this way, we can see that the destructive effect of gamma radiation on multi-component optical systems through caps protection is less reduced compared to the one for protons. From Fig. 1 can be seen that a protective cover of 10mm placed in front of multi-component system will reduce the initial dose rate which affects the first component of the optical system by about 13%. In this paper we analyzed the effect of sample thickness on laser parameters. We found an effect of laser beam auto-focus with increasing the sample thickness, the waist movement position (comparable to the thickness of the sample), a narrowing of the Rayleigh length and an increase in the divergence angle. In the case of TEMPAX samples, with a thickness of 5 times lower (2mm), this phenomenon is

negligible. In addition, the analogy between protons and neutrons effects in these types of samples, and the presence of boron (neutron absorption cross sections very high and a percentage of boron of about 13%) make borosilicate type glasses protection appropriate to be used when working in neutrons rich environments [8].

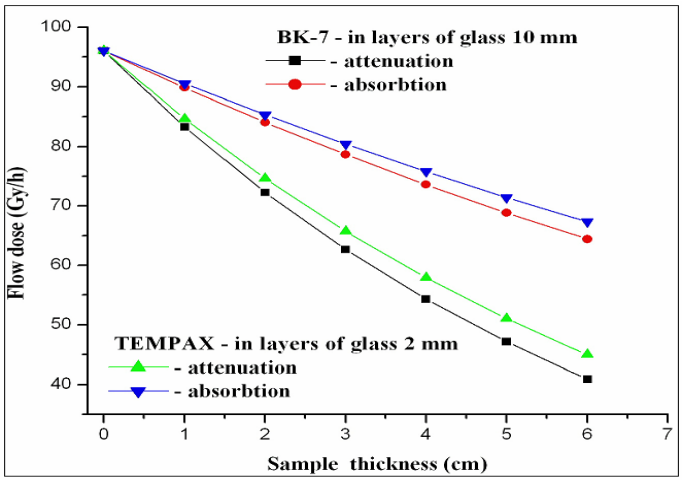

Fig.1 – The dose flow as a function of sample thickness.

After irradiation, the main change induced in the glass structure consists in the creation of stable and meta-stable defects or changes of the connections of valence electrons from the glass network (atoms or impurities). Some of this electronic configuration changes or other defects, cause preferentially light absorption. For this reason, the glass became colored and therefore these defects are called color centers. Due to the numerous applications of this material, we investigated the changes of optical parameters induced by ionizing radiation. Tests were done on two varieties of optical glass used in laser and nuclear technology. BK7 glass samples have cylindrical form, with a diameter of 25 mm and a thickness of 10 mm, and Tempax glass have a flat parallelepiped form, a surface of (10×10) mm^2 and a thickness of 2 mm.

The samples were exposed to gamma radiation at a dose of 24.4 kGy (t = 34°C) and to protons at an approximately 36 kGy dose (t = 40°C). The irradiation at different temperatures aimed the effect of dose uniformity. BK7 and Tempax types glass samples were irradiated to protons at the DFN Tandem Van de Graaf 9MV accelerator facility (IFIN-HH), and to gamma radiations at IRASM Technology Center (IFIN-HH), using a ^{60}Co source.

For the 12MeV energy protons irradiation it was taken into account the possibility of activating the samples. After irradiation, gamma spectra were taken for samples. In Fig. 2 and Fig. 3 it is show the gamma spectra of the protons irradiated BK-7and, respectively, Tempax samples.

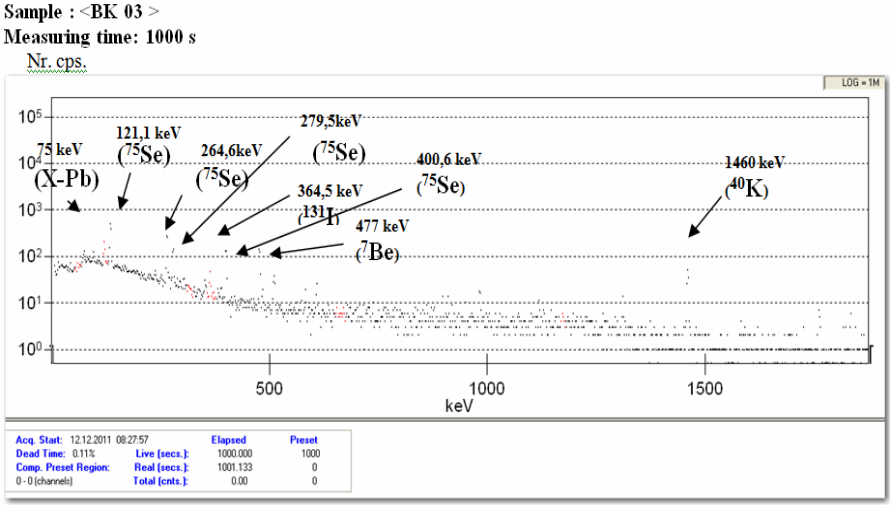

Fig. 2 – Gamma spectra of BK-7 irradiated samples.

From both graphs it is observed that the most pronounced peaks, compared to the background, have low levels of activity (in cps), induced by protons with energy of 12MeV. To this has contributed the use of about 5nA current intensities for the protons beam, which resulted of carrying a small number of particles (3×10^{10}). The maximum activity of the samples (in counts per second – cps) is between 10^2cps for TEMPAX and 10^3cps for BK. For radioprotection reasons, these samples were measured after a 30 days period, in which the values of induced activity were reduced to almost zero.

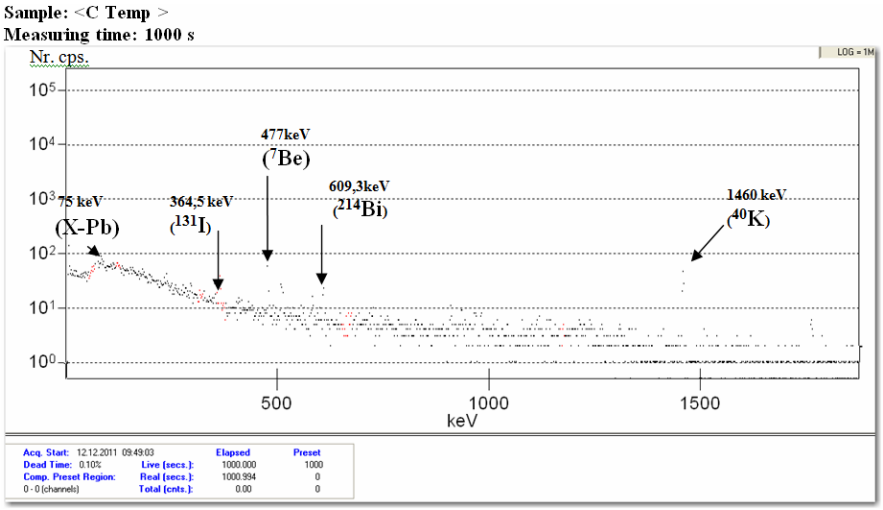

Fig. 3 – Gamma spectra of TEMPAX irradiated samples.

2. EXPERIMENTAL MEASUREMENTS OF THE ENERGETIC AND SPATIAL PARAMETERS OF THE LASER BEAM AFTER PASSING THROUGH THE SAMPLES

2.1. THE POWER TRANSMITTED THROUGH THE GLASS SAMPLES

Measurement of the transmitted laser power through the air, through non irradiated and through irradiated samples (gamma and proton) was performed for two types of glass. The experimental set-up used it is shown in Fig.4. The results are presented in Table 2. For the BK-7-type samples were observed relative variations to the initial laser power (in air) of: 7% (blank), 88% (24.4 kGy-gamma) and 18% (protons). For the Tempax type samples, relative variations to the air are: 6% (blank), 17% (24.4 kGy-gamma), and 24% (36 kGy-protons). The laser power transmitted through the samples was measured with a Coherent power meter USB type PM30.

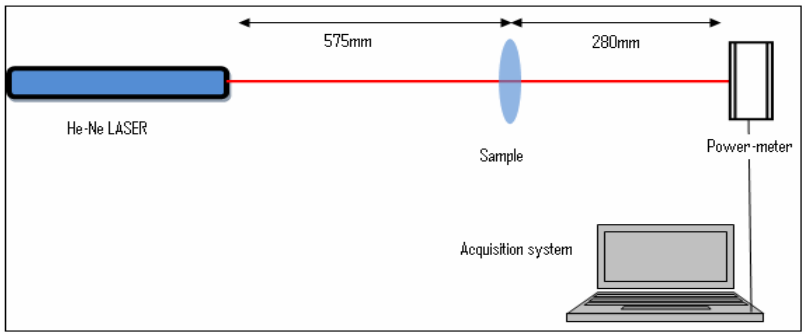

Fig. 4 – A schematic diagram of the measuring system of the power transmitted through the samples.

Table 2

The transmitted power through the sample values and their relative variations to the air

Glass type		Dose (kGy)			
		0 (air)	0	24.4	36
BK-7 gamma	Mean Power (mW)	14.17 ±2.6%	13.21±2.8% -6.78% (relative variation vs. air)	1.74±2.2% -87.91% (relative variation vs. air)	
BK-7 protons					11.65±3.2% -17.78% (relative variation vs. air)
TEMPAX gamma			13.38±2.7% -5.58% (relative variation vs. air)	11.79±3.1% -16.80% (relative variation vs. air)	
TEMPAX protons					10.80±3.5% -23.78% (relative variation vs. air)

The laser beam energy characteristics measurements are regulated by ISO 11654 [9]. In Fig. 5 it is presented, as an example, the initial value of the laser beam power (in air) and the stability of this value over a period of time of 35 minutes.

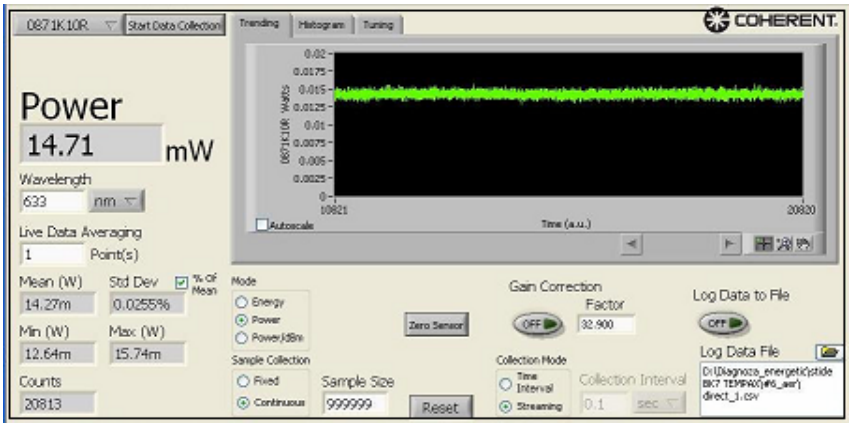

Fig. 5 – Example of measuring the maximum power transmitted through the air and its stability during 35 minutes.

2.2. CHECKING THE GAUSSIAN NATURE OF THE LASER BEAM WHEN PROPAGATE THROUGH THE TEST SAMPLES

Checking the Gaussian nature of the beam (artificial, real) was done by calculating two parameters, which are astigmatism and asymmetry according to relations, 3 and 4 [10]. Table 5 shows the variation of asymmetry and astigmatism for the two types of samples for the artificial beam and Table 6 for the real one.

The astigmatism and asymmetry values (along with the Rayleigh range) are not covered by the ISO procedure, but are provided as auxiliary values that may be of use, depending on your laser and individual concerns. The astigmatism result is an attempt to provide a figure of the beam quality factor that indicates the presence and the magnitude of axis astigmatism. Equation 3 shows the astigmatism expression:

$$a = \frac{\left|Z_{02x} - Z_{02y}\right|}{\left(Z_{R02x} + Z_{R02y}\right) \times 0.5}. \tag{3}$$

The equation that defines this value, used by us, may or may not agree with other conventions that may be in use. Equation 4 shows the asymetry expression:

$$a' = \max\left\{\left(\frac{D_{02x}}{D_{02y}}\right)_i\right\} = \max\left\{\left(\frac{D_{02y}}{D_{02x}}\right)_i\right\}. \tag{4}$$

The asymmetry results provide an indication of how circular the laser beam might be. This value compares the two waist widths only, and therefore only has significance if the laser contains little or no astigmatism. Values greater than 1 indicate greater amounts of ellipticity, or asymmetric behavior.

2.3. LASER BEAM SPATIAL PARAMETERS AFTER PASSING THROUGH THE SAMPLE (BEFORE AND AFTER IRRADIATION)

The International Standard ISO 11146 [11] refers to the measurement of spatial parameters of laser beam having rotational or orthogonal symmetry. Parameters that can be measured or calculated are: cross-sectional dimensions of the beam (second order moments) –dσ(*z*), waist position–Z_{0i}, Rayleigh length–Z_{R0i}, divergence angle–Θ_{0i} and beam quality factor M^2. The value of (*i*) depends on how the parameters are measured or calculated, meaning the laser beam artificial-after focusing ($i = 2$) or the real-before focusing ($i = 1$). Additionally two more parameters were calculated asymmetry and astigmatism, which give information about the laser beam nature, keeping or not keeping the Gaussian nature before and after passing through a medium disturbed by external factors (*i.e.* nuclear radiation). For measurement, the experimental technique assume that a fraction of the beam to be directed toward the focusing lens and CCD camera beam analyzer, using a mirror and an optical wedge, and passing through the irradiated sample and neutral filters having the porpoise of attenuate the initial beam. CCD beam analyzer (GRAS 20 Spiricon-Ophir) is mounted on a linear rail, which allows the measurement of transverse spatial beam profile (density distribution of the laser energy) at different propagation distances –*Z* known. Beam absorbers adapt the power density of the beam to be analyzed, according to the limitation conditions required by the CCD.

To measure spatial propagation parameters, the beam is focused with a converging lens with the position and parameters known ($f = (281.8 \pm 5\%)$ mm, 633nm, CVI type PLCX -50) and then measuring the diameter of the beam dσ(*z*) after the focusing lens with the CCD beam analyzer at different propagation distances *Z* from the rear principal plane of the lens (artificial beam). For lower uncertainties, fitting of experimental data was performed with a different propagation equation than the one recommended by the ISO:

$$d\sigma(z) = d\sigma(0)\{1 + [(z - z_0)/z_R]^2\}^{0.5}. \quad (5)$$

The paper has studied the influence of the color centers induced in our samples by two different types of radiation (protons and gamma) on the propagation characteristics of the laser beam after passing through the irradiated and non-irradiated samples but also on the shape of the spatial profile of the irradiation. The results are very important in applications for the production of laser beams with different propagation characteristics or operating in environments affected by nuclear radiation. Measurements were made both in stigmatic laser

beam approximation (circular distribution of power density in the transversal *Z* direction), and in simple astigmatic laser beam approximation (elliptical power density distribution). Measurements of the spatial parameters of He-Ne laser beam in air and after introducing of irradiated or non-irradiated samples were performed using the experimental set-up from Fig. 6, additional data being contained in the papers [12, 13, 14, 15, 16].

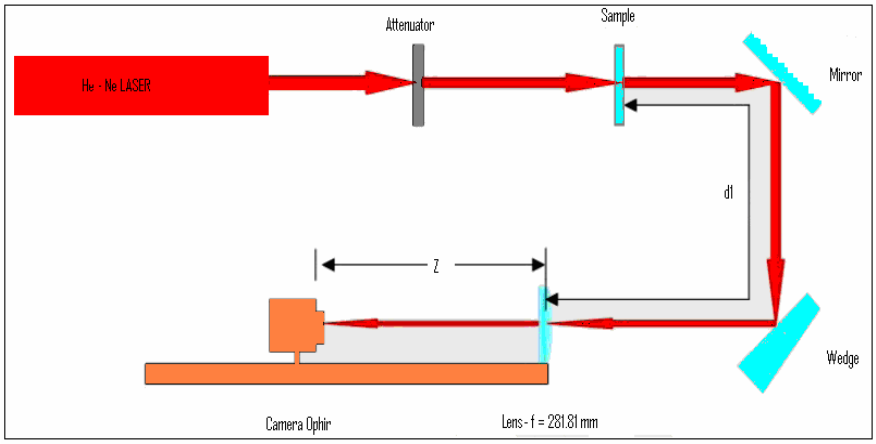

Fig. 6 – The experimental setup used to measure the spatial parameters of the laser beam after passing through the irradiated samples.

3. RESULTS AND DISCUSSION

3.1. CHECKING THE GAUSSIAN NATURE OF THE BEAM

Tables 3 and 4 show the astigmatism and asymmetry values for equations (3) and (4) to artificial and real beam.

Table 3

Variation of asymmetry and astigmatism for the two types of samples for the artificial beam

	TEMPAX		BK – 7	
Dose (kGy)	Astigmatism	Asymmetry	Astigmatism	Asymmetry
air	0.10602	1.01493	0.10602	1.01493
0	0.01907	0.96403	0.13749	1.01098
24.4 -gamma	**0.18747**	1.03053	**0.16804**	1.0202
36 - protons	0.01685	1	0.16997	0.98969
Variation vr. air (%)	**43.45**	1.51	**37.62**	0.52

Table 4

Variation of asymmetry and astigmatism for the two types of samples for the real beam

TEMPAX			BK – 7	
Dose (kGy)	Astigmatism	Asymmetry	Astigmatism	Asymmetry
air	0.05299	1.03226	0.10917	1.03226
0	0.00683	0.93939	0.01318	1
24.4 -gamma	**0.14469**	1.03333	**0.31311**	1.05238
36 - protons	0.03614	1	0.07269	0.625
Variation vr.air (%)	**63.38**	0.13	**65.13**	1.91

The results from this equation (Table 3 and Table 4 (col. 2 and col. 4)) are values between 0 and 1which indicate a laser with an increasing degrees of astigmatism, but the two waist locations are each contained within each other's Rayleigh range.

Asymmetry values will approach one, indicating that the laser appears circular in the waist region (Table 3 and Table 4 (col. 3 and col. 5)). Additionally, it is observed that the largest variation of astigmatism (lin. 5 in both tables) for both types of glasses and type of gathering (artificial and real) is the gamma rays (24.4 kGy). The variation of the asymmetry of the beam, in all cases is less than 2%, thus negligible. In this way initially maintain the Gaussian laser beam and its propagation through the samples.

3.2. LASER BEAM SPATIAL PARAMETERS AFTER PASSING THROUGH THE SAMPLE

The measured beam diameters data at various positions along the lens created waist are given in Fig. 7. Numerical values for the beam parameters (Z_{02}, Z_{R2}, d_{02}) were direct obtained by fitting to theoretical relation given in eq. 5 and indirect calculation for M^2, θ_2 parameters. The results of these calculations are given in Table 5 (A, C) for stigmatic laser beam and Table 6 (A_1, C_1) for simple astigmatic beam. In addition, based on these parameters determined by the focusing lens were determined and the actual beam parameters before her. The results of these calculations are given in Table 5 (B, D) for stigmatic laser beam and Table 6 (B_1, D_1) for simple astigmatic beam. The analysis columns (7, 8) of these table shows that relative variations *versus* air have no signifying variations on any parameters for both types of samples.

In comparison with the TEMPAX glass samples, for the BK-7 glass samples we can observe auto-focus process (a decrease in the diameter of the beam), an increase in the waist position location, a shorter Rayleigh length and an increased divergence angle. These effects are visible in Fig. 7.

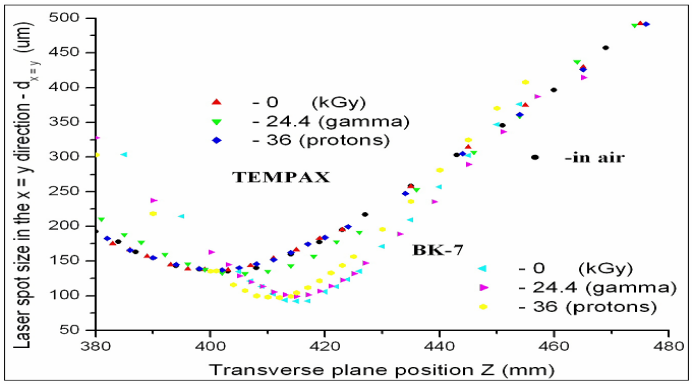

Fig. 7 – The beam diameter variation depending on the position of the plane perpendicular to the direction of propagation – *Z* for our four situations in which the samples were measured (air, non-irradiated, 24.4 kGy gamma irradiated and, respectively, 36 kGy protons irradiated).

After focusing lens, using irradiated and no irradiated samples, the nearest area Gaussian profile is in the waist. Knowing the physical parameters determined by focusing the beam for the two types of samples can then calculate the physical parameters related to provision the original beam (real) before focusing. Must be checked if we are interested to see if the laser beam maintain its initial parameters after passage through different media and through free space propagation. The results are shown in Table 5 and Table 6.

Additional information on Gaussian beam propagation can be provide by studying the evolution of the measured radius of curvature of the artificial laser beam (stigmatic) in air, to blank glasses, to the 24.4 kGy gamma dose irradiated samples, and to the ones at 36 kGy, as a function of propagation positions for distance *Z* for both TEMPAX and BK-7 glass:

$$R(Z)_i = Z_i - Z_{0i} + \frac{Z_{Ri}^2}{Z_i - Z_{0i}}, \tag{4}$$

where i – parameter referring to the beam propagation in: air, blank samples, 24.4 kGy gamma dose irradiated samples, and 36 kGy protons dose irradiated samples.

$R(Z)_i$, showed in Fig. 8, is the radius of curvature of the wave-front at positions Z_i on the laser beam axis. As illustrated here, the radius of curvature is infinite at $Z_i=Z_{0i}+Z_{Ri}$, corresponding to planar wave-fronts. It decreases to a minimum value of $2\times Z_{Ri}$ at this point. This is the point at which the wave-front has the greatest curvature. For negative *Z* the wave-fronts follow an identical pattern, except for a change in sign. We have adopted the convention that a divergent wave-front has a positive radius of curvature, whereas a converging wave front has a negative radius of curvature.

Table 5

Shows parameters defining stigmatic laser beam after/before focusing - (BK-7 and TEMPAX glass)

Material Type	Dose (kGy)	Air	0	24.4 gamma	36 protons	Gamma and proton relative variation vs. air (%)	
Borosilicate BK-7 glass after focusing (A)	M^2	1.08±1.31%	1.1±1.4%	1.08±1.24%	1.09±2.2%	0±2.23%	0.93±2.88%
	Z_{R2} (mm)	20.96±0.7%	9.53±1.7%	11.58±3.24%	10.62±1.1%	-44.75±1.75%	-49.33±1.48%
	$Z_{0,2}$ (mm)	401.37±0.3%	415.45±0.09%	414.98±0.07%	411.98±0.02%	3.39±0.43%	2.64±0.42%
	θ_2(mrd)	6.45±0.89%	9.66±2.3%	8.67±4.19%	9.98±1.4%	34.42±2.53%	54.73±1.88%
	$d_{0,2}$ (mm)	0.135±0.55%	0.092±1.4%	0.1±2.67%	0.096±0.9%	-25.93±1.84%	-28.89±1.19%
Borosilicate BK-7 glass before focusing (B)	M^2	1.08±1.31%	1.1±1.4%	1.08±1.24%	1.09±2.2%	0±2.23%	0.93±2.88%
	Z_{R1} (mm)	112.93±2.6%	42.14±2.9%	51.47±2.01%	49.21±1.5%	-54.42±4.19%	-56.42±3.97%
	$Z_{0,1}$ (mm)	926.16±1.93%	872.95±1.7%	873.61±1.77%	887.78±1.7%	-5.67±3.25%	-4.14±3.22%
	θ_1(mrd)	2.78±1.54%	4.56±2.6%	4.11±2.36%	4.21±1.9%	47.84±3.21%	51.44±2.89%
	$d_{0,1}$ (mm)	0.31±1.37%	0.19±1.9%	0.21±1.92%	0.21±1.5%	-32.26±2.73%	-32.26±2.45%
Borosilicate TEMPAX glass after focusing (C)	M^2	1.08±1.31%	1.08±1.4%	1.1±2.29%	1.07±0.8%	1.85±3.5%	-0.93±2.45%
	Z_{R2} (mm)	20.96±0.7%	21.50±0.7%	20.17±1.19%	21.96±0.4%	-3.77±0.95%	4.7±2.03%
	$Z_{0,2}$ (mm)	401.37±0.3%	400.61±0.03%	403.28±0.05%	400.42±0.05%	0.48±1.55%	-0.24±1.07%
	θ_2(mrd)	6.45±0.89%	6.37±0.95%	6.64±1.54%	6.28±0.5%	2.95±0.43%	-2.64±0.43%
	$d_{0,2}$ (mm)	0.135±0.55%	0.137±0.6%	0.134±0.98%	0.138±0.3%	-0.74±1.91%	2.22±1.24%
Borosilicate TEMPAX glass laser before focusing (D)	M^2	1.08±1.31%	1.08±1.4%	1.1±2.29%	1.07±0.8%	1.85±1.25%	-0.93±0.83%
	Z_{R1} (mm)	112.93±2.6%	117.09±2.6%	105.64±2.76%	119.75±2.5%	-6.46±2.02%	6.04±2.02%
	$Z_{0,1}$ (mm)	926.16±1.93%	928.98±1.9%	917.97±1.91%	929.10±1.9%	-0.88±3.33%	0.32±3.33%
	θ_1(mrd)	2.78±1.54%	2.73±1.5%	2.90±1.98%	2.68±1.4%	4.32±2.59%	-3.6±2.59%
	$d_{0,1}$ (mm)	0.31±1.37%	0.32±1.3%	0.31±1.58%	0.32±0.3%	0±1.96%	3.23±1.96%

Figure 8 shows illustration of the measured radius of curvature evolution of the artificial laser beam (stigmatic) in air, to blank glasses, to the 24.4kGy gamma dose, and to the 36 kGy dose of protons, as a function of propagation distance –*Z* for both TEMPAX and BK-7 glass.

Comparing the two images associated with the two types of samples (Fig. 8) it is showed the influence of BK-7 glass sample thickness on the beam wave-front propagation, for different positions according to the direction of its axis of propagation –*Z*.

Table 6

Shows parameters defining simple astigmatic laser beam after/before focusing custom perpendicular directions *x* and *y*

Material Type	**Dose (kG)**	**Air**	**0**	**24.4**	**36**	**Gamma and proton relative variation vs. air (%)**	
Borosilicate BK-7-glass after focusing (A_1)	M^2_x	1.08±1.17%	1.1±1.65%	1.07±1.11%	1.08±1.29%	-0.93±1.99%	0±2.1%
	M^2_y	1.08±1.60%	1.1±1.38%	1.08±1.43%	1.09±1.29%	0±2.68%	0..93±2.6%
	Z_{R2x}	21.38±0.63%	9.61±1.87%	11.88±1.19%	10.53±1.14%	-44.43±1.48%	-50.75±1.45%
	Z_{R2y}	20.50±0.85%	9.30±1.73%	11.21±1.32%	10.65±1.14%	-45.32±1.79%	-48.05±1.66%
	$Z_{0,2x}$	400.15±0.02%	414.80±0.03%	413.98±0.07%	412.88±0.02%	3.46±0.08%	3.18±0.03%
	$Z_{0,2y}$	402.37±0.03%	416.10±0.03%	415.92±0.07%	411.08±0.23%	3.37±0.08%	2.17±0.23%
	$d_{0,2x}$	0.136±0.50%	0.092±1.57%	0.101±2.21%	0.096±0.98%	-25.74±2.32%	-29.41±1.21%
	$d_{0,2y}$	0.134±0.68%	0.091±1.45%	0.099±2.75%	0.097±0.89%	-26.12±2.9%	-27.61±1.28%
	θ_{2x}	6.38±0.80%	9.56±2.44%	8.52±2.12%	9.08±1.54%	33.54±2.4%	42.32±1.91%
	θ_{2y}	6.53±1.09%	9.76±2.26%	8.81±2.31%	9.08±1.54%	34.92±2.78%	39.05±2.18%

Table (Continued)

Borosilicate BK-7-glass before focusing (B_1)	M^2_x	1.08±1.17%	1.1±1.65%	1.07±1.11%	1.08±2.29%	-0.93±1.99%	0±2.83%
	M^2_y	1.08±1.60%	1.1±1.38%	1.08±1.43%	1.09±2.29%	0±2.68%	0.93±3.22%
	Z_{R1x}	116.66±0.63%	42.93±1.87%	53.56±1.98%	48.35±1.14%	-54.09±2.17%	-58.56±1.45%
	Z_{R1y}	109.79±0.85%	40.73±1.73%	49.15±1.32%	50.25±1.14%	-55.23±1.79%	-54.23±1.66%
	$Z_{0,1x}$	929.63±0.02%	875.77±0.03%	877.79±0.07%	883.73±0.02%	-5.78±0.08%	-4.94±0.03%
	$Z_{0,1y}$	923.63±0.03%	870.27±0.03%	869.78±0.07%	891.95±0.2%	-5.83±0.08%	-3.43±0.23%
	$d_{0,1x}$	0.32±0.5%	0.19±1.57%	0.221±2.21%	0.20±0.98%	-31.25±2.32%	-37.5±1.2%
	$d_{0,1y}$	0.31±0.7%	0.19±1.45%	0.21±2.75%	0.21±0.98%	-32.26±2.91%	-32.26±1.37%
	θ_{1x}	2.73±0.8%	4.52±2.44%	4.01±1.12%	4.24±1.5 4%	46.89±1.59%	55.31±1.91%
	θ_{1y}	2.83±1.01%	4.67±2.26%	4.21±1.31%	4.18±1.55%	48.76±2.02%	47.7±2.19%
Borosilicate TEMPAX glass after focusing (C_1)	M^2_x	1.08±1.17%	1.08±1.16%	1.08±1.94&	1.07±0.82%	0±2.55%	-0.93±1.85%
	M^2_y	1.08±1.60%	1.08±1.72%	1.11±2.84%	1.08±0.77%	2.78±3.63%	0±2.39%
	Z_{R2x}	21.38±0.63%	20.75±0.60%	21.10±1.02%	21.96±0.43%	-1.35±1.57%	2.71±0.99%
	Z_{R2y}	20.50±0.85%	22.25±0.90%	19.12±1.46%	21.96±0.40%	-6.73±1.89%	7.12±1.27%
	$Z_{0,2x}$	400.15±0.02%	400.81±0.04%	401.27±0.04%	400.84±0.02%	0.28±0.05%	0.17±0.03%
	$Z_{0,2y}$	402.37±0.03%	400.40±0.04%	405.04±0.05%	401.26±0.02%	0.66±0.07%	-0.28±0.05%
	$d_{0,2x}$	0.136±0.50%	0.134±0.50%	0.135±0.83%	0.138±0.35%	-0.74±1.09%	1.47±0.79%
	$d_{0,2y}$	0.134±0.68%	0.139±0.73%	0.131±1.22%	0.13±0.33%	2.24±1.55%	2.99±1.02%
	θ_{2x}	6.38±0.80%	6.46±0.75%	6.41±1.31%	6.28±0.56%	0.47±1.73%	1.57±1.26%
	θ_{2y}	6.53±1.09%	6.27±1.16%	6.86±1.90%	6.30±0.52%	5.05±2.45%	-352±1.63%
Borosilicate TEMPAX glass before focusing (D_1)	M^2_x	1.08±1.17%	1.08±1.16%	1.08±1.94&	1.07±0.82%	0±2.55%	-0.93±1.85%
	M^2_y	1.08±1.60%	1.08±1.72%	1.11±2.84%	1.08±0.77%	2.78±3.63%	0±2.39%
	Z_{R1x}	116.66±2.59%	112.91±2.58%	113.86±2.71%	119.75±2.58%	-2.4±4.56%	2.65±4.48%
	Z_{R1y}	109.79±2.63%	121.35±2.67%	97.63±2.87%	118.2±2.53%	-11.08±4.7%	7.68±4.5%
	$Z_{0,1x}$	929.63±1.94%	929.39±1.94%	926.38±1.94%	929.10±1.94%	-0.36±3.36%	-0.06±3.36%
	$Z_{0,1y}$	923.63±1.92%	928.59±1.95%	911.00±1.89%	924.80±1.92%	-1.37±3.31%	0.13±3.32%
	$d_{0,1x}$	0.32±1.35%	0.31±1.35%	0.31±1.50%	0.32±1.35%	-3.13±2.43%	0±2.34%
	$d_{0,1y}$	0.31±1.42%	0.33±1.46%	0.30±1.74%	0.32±1.29%	-3.23±2.66%	3.23±2.39%
	θ_{1x}	2.73±1.49%	2.77±1.48%	2.76±1.82%	2.68±1.47%	1.17±2.74%	-1.83±2.57%
	θ_{1y}	2.83±1.65%	2.6±1.71%	3.03±2.27%	2.71±1.35%	7.07±3.26%	-4.24±2.7%

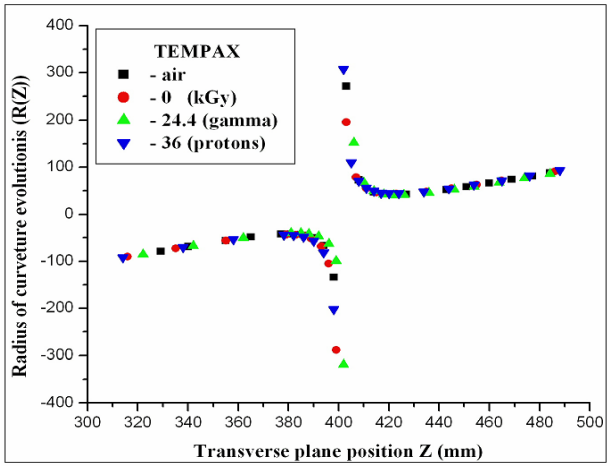

Fig. 8a – Illustration of the measured radius of curvature evolution of the artificial laser beam (stigmatic) in air, to blank glasses, to the 24.4 kGy gamma dose, and to the 36 kGy dose of protons as a function of propagation distance –Z for TEMPAX glass.

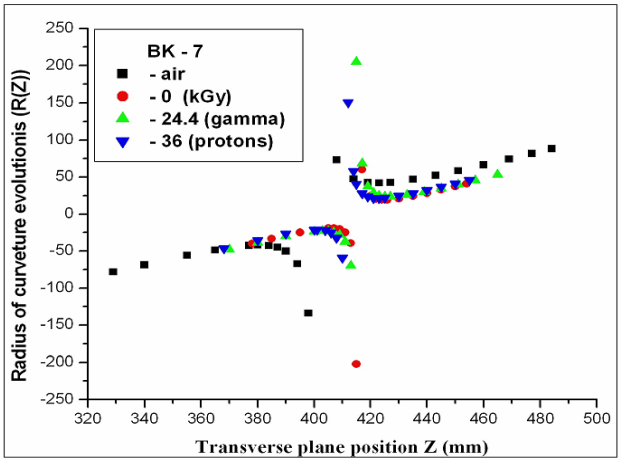

Fig. 8b – Illustration of the measured radius of curvature evolution of the artificial laser beam (stigmatic) in air, to blank glasses, to the 24.4 kGy gamma dose, and to the 36 kGy dose of protons as a function of propagation distance –*Z* for BK-7 glass.

4. CONCLUSIONS

We performed a series of tests by measuring the spatial propagation parameters for a continuous wave laser beam. The tests were carried out on a standard He-Ne laser in accordance with ISO 11146 –1 2005. Some parameters studied regarding the propagation of the beam after passing through blank sample and the ones irradiated with gamma and protons, have been obtained directly from the experimental data hyperbolic fitting and others were calculated. The analysis of the experimental data provided by these tests showed that the values obtained by the method of fitting had a relative uncertainty of less than 5%, and that for the 633nm wavelength and dose values taken into account, no significant variation of determined parameters was observed. For each type of glass, for both photon and proton, the changes of the propagation parameters are similar and have values within the limits of measurement uncertainty. Only the different thickness of the samples modifies certain propagation parameters but retains similar effect given by the two different types of radiation. We notice a change in the value of power transmitted through the samples, which will need to be compensated. Within certain limits, it is possible to use these types of glass to protect optical systems operating in ionizing radiation environments (gamma, proton, neutron or mixed). Test beam still retains the Gaussian profile even after passage through our irradiated samples affected (asymmetry was about one and astigmatism was very close to zero). The maximum difference of astigmatism for the two types of samples is about 6% for artificial beam (after focusing) and 2% real beam (before focusing).

Acknowledgements. We would like to thank to Dr. G. Nemeş and Dr. A. Stratan, ISOTEST Laboratory, National Institute for Lasers, Plasma and Radiation Physics for optical measurements and discussion. Similar thanks to the Irradiation Technology Center IRASM-IFIN-HH for providing technical support for irradiations.

REFERENCES

1. M. F. Bartusiak, J. Becher, *Proton-induced coloring of multicomponent glasses*, Applied Optics, **18**, *19* (1979).
2. T. Jensen, B. R.Lawn, R. L.Dalglish, J. C.Kelly, *Surface Cracking in proton-irradiated Glass*, Radiation Effects, **28**, 245–247 (1976).
3. www.srim.org./TRIM/SRIM2008
4. A. K.Sandhu, S. Singh, O. P. Pandy, *Gamma ray induced modifications of quaternary silicate glasses*, Journal of Physics**, 41** (2008).
5. S. Baccaro, A. Piegari, I. Di. Sarcina, A. Cecilia, *Effect of gamma irradiation on optical components*, IEEE Transmission on Nuclear Science, **52**, *5* (2005).
6. A. Gusarov, D. Doyle, L. Glebov, F. Berghamans, *Comparison of radiation-induced transmission degradation of borosilicate crown optical glass from four different manufactures*, Photonics for Space Environments X, Proceeding of SPIE, **5897**, 2005.
7. www.nist.gov
8. M. R. Ioan, I. Gruia, P. Ioan, M. Bacalum, G. V. Ioan, C. Gavrila, *3MeV protons to simulate the effects caused by neutrons in optical materials with low metal impurities*, J. Optoelectron. Adv. Mater., **15**, *5–6*, 523–529 (2013).
9. ISO 13654, *Test methods for laser beam parameters*: *Power* (*energy*) *density distribution*.
10. www.ophiropt.com**.**
11. ISO 11146, *Test methods for laser beam parameters*: *Beam widths*, *divergence angle and beam propagation factor*.
12. M. R. Ioan, I. Gruia, P. Ioan, I. L. Cazan, C. Gavrila, *Investigation of optical effects induced by gamma radiation in refractory elements*, J. Optoelectron. Adv. Mater., **15**, *3–4*, 254 (2013).
13. M. R. Ioan, I. Gruia, G. V. Ioan, L. Rusen, P. Ioan, A. Zorila, *Laser beam evaluation methods to study changes in 12 MeVenergetic proton irradiated glasses*, J. Optoelectron. Adv. Mater., **15**, *11–12*, 1403–1411 (2013).
14. D. M. Keicher, *Laser beam Characterization Results for a High Power CW Nd: YAG Laser*, SPIE Proceedings, **2375**, pp. 161–171 (1995).
15. J. V. Sheldakova, A. V. Kudryashov, V. Y. Zavarova, T. Y. Cherezova, *Beam quality measurements with Shack-Hartmann wave front sensor and M^2-sensor: comparasion of two methods*, SPIE Proceedings, **6452** (2007).
16. M. R. Ioan, I. Gruia, G. V. Ioan, L. Rusen, P. Ioan, *Laser beam used to measure and highlight the transparency changes in gamma irradiated borosilicate glass*, Journal of Optoelectronics and Advanced Materials, **16**, *1–2*, 162–169 (2014).